Nuclear equation of state with momentum-dependent interactions

László P. Csernai,[1,5] George Fai,[2] Charles Gale,[3] and Eivind Osnes[4,5]
[1] *Physics Department, University of Bergen, N-5007 Bergen, Norway*
[2] *Department of Physics, Kent State University, Kent, Ohio 44242*
[3] *Physics Department, McGill University, Montreal, Quebec, Canada H3A 2T8*
[4] *Physics Department, University of Oslo, P.O. Box 1048, N-0316 Oslo 3, Norway*
[5] *Theoretical Physics Institute, University of Minnesota, Minneapolis, Minnesota 55455*
(Received 16 September 1991)

The nuclear-matter equation of state is studied with a momentum-dependent effective interaction. The incompressibility and the zero-temperature optical potential are calculated analytically. The momentum distribution of nucleons is examined and the effect of the momentum dependence on pion-production rates is illustrated. The phase transition to a quark-gluon plasma, described by a bag-model equation of state, is studied in an approximation suitable for infinite nuclear matter.

PACS number(s): 25.75.+r, 21.65.+f

I. INTRODUCTION

The equation of state (EOS) of strongly interacting matter has become a major focus of nuclear theory research in the past decade. The interest is partly due to implications and connections beyond standard nuclear physics, such as astrophysical consequences (early Universe, neutron stars, supernovae) and the interface with the physics of the underlying quark-gluon degrees of freedom. In the present work we examine the effect of the momentum dependence of the nucleon mean field on the assumed phase transition to a quark-gluon plasma (QGP). We work with a simple effective interaction, the momentum-dependent Yukawa interaction, which is widely used in the literature and will be introduced in Sec. II. We emphasize that the goal of this work is not to provide a theory of nuclear matter starting from a realistic interaction; rather, we study the equilibrium properties of a simple momentum-dependent effective interaction, which is frequently used in dynamical situations.

The EOS efficiently summarizes information on globally static, infinite nuclear matter in a wide density and temperature interval. The incompressibility of nuclear matter and phase transition properties are frequently used as the most simple indicators of the EOS. While the idealized situation referred to by the EOS can only be approximated in actual nuclear collisions and the outcome of collision experiments will depend on many other factors (e.g. time scales and the transport properties of the medium), the availability and planning of facilities to probe the nuclear EOS gives continuing stimulus to the EOS research.

Traditionally, the incompressibility of nuclear matter, K (see Sec. III C for a definition), has been extracted from the giant monopole resonance (breathing mode) [1, 2]. As nuclear collision data became available [3], several groups started to use transport theoretical models based on the Boltzmann equation to obtain related information [4, 5]. The nuclear mean field is an input to these calculations. Applying a momentum-independent mean field, it was first reported that a stiff EOS ($K \approx 380$ MeV) provided a better fit to certain data (e.g., pion yields and collective sidewards flow), than a soft ($K \approx 200$ MeV) one [5]. This appeared to contradict supernova calculations requiring a rather soft EOS [6, 7] and subsequent Fermi-liquid calculations giving a low incompressibility of nuclear matter [8], and led to the introduction of momentum-dependent mean fields (which generally lower K) in transport model calculations [9–11].

It needs to be emphasized that the study of the EOS has grown into a flourishing field of research, where a large number of investigators use different approaches from statistical models to microscopic calculations [12]. Here we can only mention a few developments, most relevant from our perspective.

Since their inception, momentum-dependent mean fields play an increasing role in the EOS calculations (see, e.g., Ref. [13]). The momentum dependence has important implications on the static and dynamic properties of nuclear matter. An example of this, the effect on the incompressibility [14, 15], was mentioned above. In addition, the momentum distribution of the nucleons at finite temperature will be more complicated than a Maxwell-Boltzmann distribution (in the classical limit) in the presence of a momentum-dependent mean field. This may change production cross sections of recent interest [16, 17].

In the present work, we focus on the momentum distribution in a momentum-dependent mean field and on the QGP phase transition. We use a parametrization of the mean field which gives a satisfactory fit to (zero-temperature) optical potentials to rather high bombarding energies. We introduce an equivalent mass, which can be used in an approximate Maxwell-Boltzmann distribution to simplify numerical calculations at sufficiently high temperature and low density. We demonstrate that the change in the momentum distribution of nucleons

induced by the momentum dependence leads to a reduction of equilibrium pion-production rates. The incompressibility is calculated analytically for a family of momentum-dependent mean fields. The EOS of hadronic matter is calculated with the help of thermodynamic perturbation theory, and the phase transition to a QGP, described by a bag-model EOS, is investigated.

In Sec. II we discuss momentum-dependent interactions in general, while in Sec. III we use the momentum-dependent Yukawa interaction (MDYI) to derive the mean-field approximation for single-particle properties, to calculate the optical potential at zero temperature, and to obtain an analytical formula for the nuclear matter incompressibility. In Sec. IV we introduce certain simplifying approximations and present the momentum distribution in a momentum-dependent mean field. We introduce an "equivalent mass" for calculational purposes and calculate pion-production rates in the equivalent-mass approximation. The connection between the equivalent mass and the usual effective mass is also discussed. Section V contains the derivation of the EOS using thermodynamical perturbation theory. Calculational details are relegated to the appendix. Section VI discusses the QGP phase transition. We end with a few concluding remarks in Sec. VII.

II. MOMENTUM-DEPENDENT INTERACTIONS

Theoretical models presently used in the description of nuclear collisions can be derived from the Boltzmann equation [18]. The single-particle distribution function $f(\mathbf{r},\mathbf{p})$, normalized to the local nucleon density as $n(\mathbf{r}) = \int d^3p\, f(\mathbf{r},\mathbf{p})$, is a basic quantity in these investigations. It is therefore desirable to express the Hamiltonian for an A-nucleon system with two-body interaction v_{ij}, three-body interaction v_{ijk}, etc.,

$$H = \sum_{i=1}^{A} \frac{p_i^2}{2m} + \frac{1}{2}\sum_{i,j=1}^{A} v_{ij} + \frac{1}{6}\sum_{i,j,k=1}^{A} v_{ijk} + \cdots , \tag{1}$$

where m is the nucleon mass, in terms of $f(\mathbf{r},\mathbf{p})$. In the present work we use a semiclassical approximation, allowing the simultaneous specification of the position $\mathbf{r}$ and the momentum $\mathbf{p}$ of the nucleons. A corresponding quantal treatment can be based on the Wigner function [19–21].

We write the energy of the system in the semiclassical Hartree approximation as

$$\begin{aligned} E &= \int d^3r\, d^3p\, \frac{p^2}{2m} f(\mathbf{r},\mathbf{p}) + \frac{1}{2}\int d^3[rpr'p'] f(\mathbf{r},\mathbf{p}) f(\mathbf{r}',\mathbf{p}')\; v_{ij}(\mathbf{r},\mathbf{r}',\mathbf{p},\mathbf{p}') + \cdots \\ &= \int d^3r d^3p\, \frac{p^2}{2m} f(\mathbf{r},\mathbf{p}) + V[f] , \end{aligned} \tag{2}$$

where $v_{ij}(\mathbf{r},\mathbf{r}',\mathbf{p},\mathbf{p}')$ is the most general two-body interaction, which depends, in addition to the positions of the two nucleons $\mathbf{r}$ and $\mathbf{r}'$, on their momenta $\mathbf{p}$ and $\mathbf{p}'$, and $d^3[rpr'p']$ represents integration over all variables in the square brackets.

It is well known that nuclear matter saturation can be achieved with density-dependent or momentum-dependent interactions, or with a combination of both. In lack of a full G-matrix calculation (which would start from a realistic free nucleon-nucleon interaction), simpler density- and momentum-dependent *effective* interactions have been used in the description of ground-state nuclear properties. The zero-range (in coordinate space) Skyrme interaction [22], offers further calculational advantages [23, 24]. Note that three-body and higher contributions are frequently represented by density-dependent terms with fractional powers of the density.

The one-body term of the energy (2) contains one distribution function, while the two-body term is obtained by convoluting the two-body interaction with two distribution functions, etc. For zero-range forces the potential energy density u contains delta-functions for the coordinates, so that one nontrivial integral over one single position coordinate $\mathbf{r}$ is left in the potential energy $V[f]$:

$$V[f] = \int d^3r\; u[f(\mathbf{r},\mathbf{p}), f(\mathbf{r},\mathbf{p}'), \ldots] . \tag{3}$$

For example, if we assume a momentum-independent nucleon-nucleon interaction, $v_{ij}(\mathbf{r},\mathbf{r}',\mathbf{p},\mathbf{p}') = v_{ij}^{(0)}(\mathbf{r}-\mathbf{r}')$, then

$$\begin{aligned} V &= \frac{1}{2}\int d^3r\, d^3p\, d^3r' d^3p'\; f(\mathbf{r},\mathbf{p}) f(\mathbf{r}',\mathbf{p}')\; v_{ij}^{(0)}(\mathbf{r}-\mathbf{r}') \\ &= \frac{1}{2}\int d^3r\, d^3r'\; n(\mathbf{r}) n(\mathbf{r}')\; v_{ij}^{(0)}(\mathbf{r}-\mathbf{r}') . \end{aligned} \tag{4}$$

Furthermore, for a zero-range momentum-independent two-body interaction,

$$v_{ij}^{(0)}(\mathbf{r}-\mathbf{r}') = \frac{a}{n_0}\delta(\mathbf{r}-\mathbf{r}') , \tag{5}$$

where n_0 is the standard nuclear matter density and a is a constant of energy dimension, the potential energy takes the form

$$\begin{aligned} V &= \frac{1}{2}\int d^3r\, d^3p\, d^3r' d^3p'\; f(\mathbf{r},\mathbf{p}) f(\mathbf{r}',\mathbf{p}') \\ &\qquad \times \frac{a}{n_0}\delta(\mathbf{r}-\mathbf{r}') \\ &= \int d^3r\; \frac{a}{2}\frac{n^2(\mathbf{r})}{n_0} . \end{aligned} \tag{6}$$

Note that the parameters of the nucleon distribution function $f(\mathbf{r},\mathbf{p})$ may also be position-dependent, e.g., the local temperature $T = T(\mathbf{r})$.

Zero-range interactions cannot be expected to ac-

curately describe, e.g., nuclear surface properties. A successful program of Thomas-Fermi calculations for ground-state properties [25–27] from the finite-range Seyler-Blanchard interaction [28] has recently been extended to study the thermostatics of finite-temperature nonuniform nuclear systems [29]. In its original version, where the entire burden of saturation was placed on the momentum dependence, the Seyler-Blanchard interaction gave a too rapid unbounded increase of the repulsion as a function of the incident energy for the zero-temperature optical potential [30]. When an explicit density dependence is introduced [27], the observed energy dependence of the optical potential can be fitted up to ≈ 200 MeV in the total energy of the incoming particle. Asymptotically the Seyler-Blanchard interaction will be dominated by the $(\mathbf{p}-\mathbf{p}')^2$ term, with increasing repulsion between particles of large relative momenta.

In the present work we focus our attention on infinite systems and high energies. We expect to have no momentum-dependent interaction at large relative momenta of the interacting nucleons. We therefore opted to use a parametrization of the momentum dependence applied recently in several heavy-ion calculations [31,32], which leads to vanishing repulsion when $|\mathbf{p}-\mathbf{p}'| \to \infty$. For the present study we consider this property more important than the ability to account for finite range effects. The form of the interaction used is motivated by the Pauli principle, and v_{ij} can be written as

$$v_{ij} = v_{ij}^{(0)}(\mathbf{r}-\mathbf{r}') + \frac{2c}{n_0}\,\frac{\delta(\mathbf{r}-\mathbf{r}')}{1+(\frac{\mathbf{p}-\mathbf{p}'}{\Lambda})^2}\,, \tag{7}$$

where c is a constant of energy dimension and Λ is a momentum range or characteristic momentum, conveniently parametrized in terms of the Fermi momentum of standard nuclear matter, $\Lambda = \lambda p_F^{(0)}$. The momentum-dependent part of the two-body interaction (7) is of zero range in coordinate space, while the momentum-independent part can be represented with either a zero-range or a finite-range effective interaction. With the zero-range form (5) and an additional three- and more-nucleon contribution for the momentum-independent part, the total energy can be written as

$$E = \int d^3r \left[\int d^3p \frac{p^2}{2m} f(\mathbf{r},\mathbf{p}) + u[f] \right], \tag{8}$$

with the potential-energy density $u[f]$ given by

$$u[f] = \frac{a}{2}\frac{n^2}{n_0} + \frac{b}{\sigma+1}\frac{n^{\sigma+1}}{n_0^{\sigma}} + \frac{c}{n_0}\int d^3p\, d^3p' \frac{f(\mathbf{r},\mathbf{p}) f(\mathbf{r},\mathbf{p}')}{1+(\frac{\mathbf{p}-\mathbf{p}'}{\Lambda})^2}\,, \tag{9}$$

where b is a constant of energy dimension and the dimensionless parameter σ can be chosen to effectively represent the three- and more-nucleon interactions. Since the second term in (7) is proportional to the Fourier transform of a Yukawa function, this interaction is referred to as momentum-dependent Yukawa interaction (MDYI). The momentum-dependent part of the MDYI has the form arising from the exchange term in a more complete (antisymmetrized) calculation, and, with the proper choice of the constant c, can be thought of as incorporating an approximate representation of the exchange effect [31]. It should be kept in mind, however, that the MDYI is of zero range in coordinate space.

III. CALCULATIONS WITH THE MDYI

Single-particle properties in the momentum-dependent mean field are often needed in practical applications. Here we derive the mean-field approximation for the MDYI in general, then analytically calculate the optical potential and the nuclear matter incompressibility at zero temperature. To achieve this we utilize the fact that the necessary integrals are analytical for a zero-temperature Fermi gas [31]. In subsequent finite-temperature applications (see Sec. IV) the Maxwell-Boltzmann approximation will be used for the thermal part of the energy.

A. Mean-field approximation

The mean-field approximation can be derived from the potential energy density u by taking the variational derivative with respect to the distribution function f,

$$\varphi \equiv \delta u[f]/\delta f(\mathbf{r},\mathbf{p})\,. \tag{10}$$

Using Eqs. (9) and (10), one obtains for the momentum-dependent part of the mean field

$$\varphi_{\rm mom}(\mathbf{r},\mathbf{p}) = \frac{2c}{n_0}\int d^3p' \frac{f(\mathbf{r},\mathbf{p}')}{1+(\frac{\mathbf{p}-\mathbf{p}'}{\Lambda})^2}\,, \tag{11}$$

hence for the momentum-dependent part of the single-particle energy

$$\varepsilon_{\rm mom}(\mathbf{r},\mathbf{p}) = \frac{p^2}{2m} + \varphi_{\rm mom}(\mathbf{r},\mathbf{p})\,. \tag{12}$$

With the parametrization of the momentum-independent part as given in Eq. (9), the full single-particle energy takes the form [10,11,31]

$$\varepsilon(\mathbf{r},\mathbf{p}) = \frac{p^2}{2m} + a\frac{n}{n_0} + b(\frac{n}{n_0})^{\sigma} + \frac{2c}{n_0}\int d^3p' \frac{f(\mathbf{r},\mathbf{p}')}{1+(\frac{\mathbf{p}-\mathbf{p}'}{\Lambda})^2}\,. \tag{13}$$

At finite temperature, $f(\mathbf{r},\mathbf{p})$ depends on the single-particle energies $\varepsilon(\mathbf{r},\mathbf{p})$, and Eq. (13) implies a self-consistency requirement. For a zero-temperature Fermi gas, the distribution is specified by the Fermi momentum, which provides an upper limit to the integral in Eq. (13). In general, the self-consistency requirement can be implemented by a numerical procedure [32]. In our simplified approximation (discussed in Sec. IV) the momentum distribution is calculated analytically, and we make further progress introducing an "equivalent-mass" approximation.

B. Optical potential at zero temperature

Using the analytical form of the integral in Eq. (13) for a zero-temperature Fermi gas, we calculated the

TABLE I. Parameters of the equations of state used in this work. Simplified MD stands for the simplified momentum-dependent interaction of Sec. IV.

EOS	a (MeV)	b (MeV)	c (MeV)	σ	λ
MDYI	-110.44	140.90	-64.95	1.24	1.58
Simplified MD	-144.90	203.30	-75.00	1.17	1.50
SBKD	-365.00	303.00		1.17	

depth of the optical potential for the MDYI for cold nuclear matter at standard density with the parameter set $a = -110.44$ MeV, $b = 140.9$ MeV, $c = -64.95$ MeV, $\sigma = 1.24$, and $\lambda = 1.58$ [31]. These parameters are fitted to yield a nuclear matter binding energy $E/A = 16$ MeV at standard density $n_0 = 0.16$ fm^{-3} and an incompressibility $K = 215$ MeV. Moreover, to fix all five parameters, the zero-temperature optical potential is required to have a value of -75 MeV at zero kinetic energy, and to vanish at 300 MeV kinetic energy. The parameters of the MDYI and other interactions used in the present work are summarized in Table I.

Figure 1 displays the calculated optical potential depth, and compares the results to available optical potential analyses. It should be kept in mind that the central depths of optical-model potentials extracted from scattering data depend on the models used in the analyses. We use this information for qualitative comparison to the MDYI results for uniform nuclear matter. In Fig. 1(a) we plot the depth of (the real part of) the optical potential as a function of the total energy of the incoming neutron, and we use an extensive compilation up to $\approx$ 200 MeV in total energy [33], against which the Seyler-Blanchard interaction was also tested [27], as a reference. In Fig. 1(b) we present the depth of the optical potential obtained with the MDYI over a wide energy range. We extend our inquiry to neutron kinetic energies up to 1 GeV, and compare to an earlier (and less detailed) standard analysis [34], and to a Dirac-equation based investigation [35]. (We will need this wide energy range for our EOS and QGP studies, see Secs. V and VI.) At high energy, the MDYI optical potential grows much slower than the ones based on different versions of the Seyler-Blanchard interaction [27], and saturates at $\approx +30$ MeV.

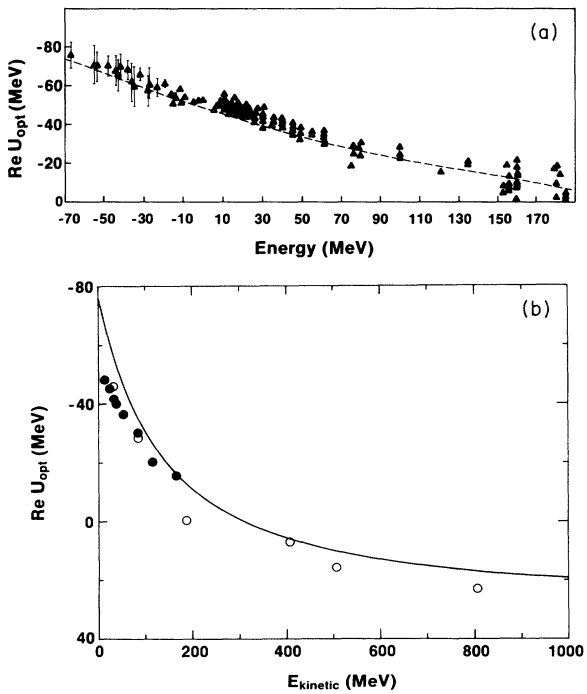

FIG. 1. The depth of the real part of the optical potential for MDYI (a) as a function of the total neutron energy at relatively low energies, and (b) as a function of the neutron kinetic energy in a wider energy range. Points are from Ref. [33] in (a), and from Ref. [34] (full dots) and Ref. [35] (open circles) in (b).

C. Incompressibility

For applications and comparisons it is frequently of interest to know the isothermal compression modulus of nuclear matter,

$$K_T = 9n \left.\frac{\partial^2 E}{\partial n^2}\right|_{T=\text{const}} . \tag{14}$$

The value of this density- and temperature-dependent quantity at standard nuclear matter density and at zero temperature is traditionally referred to as the incompressibility (or "compressibility") K of nuclear matter.

Exploiting again the analytical form of the integral in Eq. (13), it is straightforward to calculate the compression modulus at $T = 0$. The result can be written as

$$K_{T=0}(n) = 9\left[\frac{p_F^2}{3m} + a\frac{n}{n_0} + \sigma b(\frac{n}{n_0})^\sigma + c\lambda^2(\frac{n}{n_0})^{\frac{1}{3}} \times \left\{1 - \frac{\lambda^2}{4}(\frac{n}{n_0})^{\frac{2}{3}} \ln(1 + \frac{4}{\lambda^2}\frac{n_0}{n})\right\}\right], \tag{15}$$

where p_F is the Fermi momentum. For standard nuclear matter density, $n = n_0$,

$$K_{T=0}(n = n_0) = 9\left[\frac{p_F^{(0)2}}{3m} + a + \sigma b + c\lambda^2\left\{1 - \frac{\lambda^2}{4}\ln(1 + \frac{4}{\lambda^2})\right\}\right], \tag{16}$$

where $p_F^{(0)}$ stands for the Fermi momentum of standard nuclear matter.

The $T = 0$ incompressibility (15) is plotted in Fig. 2 (full line) as a function of the density with the parameter set used in Sec. III B. At standard nuclear matter density a compressibility $K = K_{T=0}(n = n_0) = 215$ MeV is obtained, as already mentioned above. For comparison, we have included the incompressibility obtained when the momentum-dependence is turned off ($c = 0$) in MDYI (dashed), and the incompressibility for the soft momentum-independent interaction referred to as SBKD

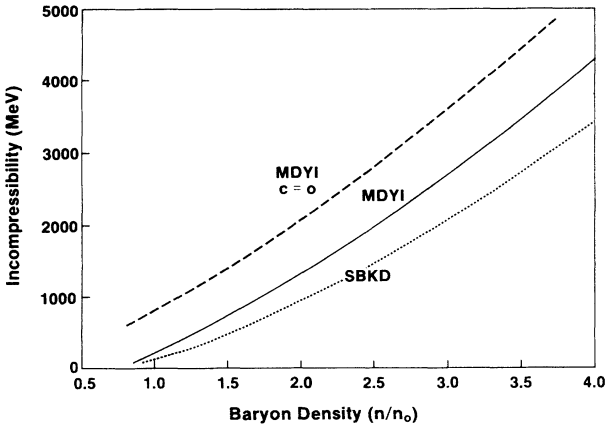

FIG. 2. The incompressibility at zero temperature as a function of the density for the MDYI (full curve), for the MDYI with the momentum dependence switched off (dashed), and for the SBKD interaction (dotted line).

(dotted line), which, except for a slight change in the value of the parameter a (yielding a softer equation of state), is the soft BKD introduced in Ref. [4] (see Table I). The SBKD interaction is used as a reference throughout the present work.

IV. SIMPLIFIED MOMENTUM DEPENDENCE FOR INFINITE NUCLEAR MATTER

A somewhat simpler momentum-dependent mean field was used in Ref. [10]. This can be obtained by replacing $\mathbf{p}'$ in the denominator of the integrand of Eq. (9) by its average, $<\mathbf{p}'>$, yielding

$$\varphi_{\rm mom}(\mathbf{r},\mathbf{p}) = \delta u[f]/\delta f(\mathbf{r},\mathbf{p}) = c\frac{n}{n_0}\left[\frac{1}{1+(\frac{\mathbf{p}-<\mathbf{p}'>}{\Lambda})^2}\right] + c\frac{n}{n_0}\left\langle\frac{1}{1+(\frac{\mathbf{p}-<\mathbf{p}'>}{\Lambda})^2}\right\rangle_p , \quad (17)$$

where $<\cdots>_p$ represents averaging with respect to the momentum p. A simple p dependence is isolated in the first term of this expression. Note, however, that the manifest symmetry between $\mathbf{p}$ and $\mathbf{p}'$, reflecting the symmetry of the nucleon-nucleon interaction [see Eq. (7)], is lost in this approximation. The use of Eq. (17) is acceptable for nuclear matter calculations, where we deal with a globally static, infinite system. However, the approximation is obviously not valid in the actual nuclear collision scenario, where the relative momentum of the two nuclei will play an important role [31,36]. For simplicity, we restrict the following considerations to the case of infinite nuclear matter. Moreover, we will assume sufficiently excited and not too dense nuclear matter in the following, so that the Maxwell-Boltzmann approximation can be used for the nucleon distribution function at a given temperature.

A. Momentum distribution

In a momentum-independent mean field, the momentum distribution in the classical limit has the usual Maxwell-Boltzmann form

$$f_0(p) = \frac{n}{(2\pi mT)^{3/2}}\exp\left[-p^2/2mT\right], \quad (18)$$

where n is the baryon density of nuclear matter. With a momentum-dependent mean field, the exponent of the momentum distribution will contain the entire momentum-dependent part of the single-particle energy [see Eq. (29)], and the corresponding distribution function will no longer be a simple Maxwellian. However, it will be advantageous for calculational purposes to *approximate* the full distribution with a Maxwellian at a given temperature and density.

In the following, we introduce an "equivalent mass," $m_{\rm eq}^{\rm MB}$ which can be used at a given temperature and density in a Maxwell-Boltzmann distribution to fit the momentum-distribution obtained with the full momentum-dependent mean field,

$$f_{\rm eq}^{\rm MB}(p) = N\exp\left[-p^2/2m_{\rm eq}^{\rm MB}T\right], \quad (19)$$

where $N = n/(2\pi m_{\rm eq}^{\rm MB}T)^{3/2}$. The equivalent mass will depend on the temperature and the density, but will be momentum-independent, $m_{\rm eq}^{\rm MB} = m_{\rm eq}^{\rm MB}(n,T)$. (The relation between the equivalent mass and the momentum-dependent effective mass will be discussed in Sec. IV B.)

As a particular example, we consider the momentum-dependent mean-field potential of Ref. [10]. The potential energy density is written as

$$u[f] = \frac{a}{2}\frac{n^2}{n_0} + \frac{b}{\sigma+1}\frac{n^{\sigma+1}}{n_0^\sigma} + c\frac{n}{n_0}\int d^3p\,\frac{f(\mathbf{p})}{1+(\frac{\mathbf{p}-\mathbf{p}_0}{\Lambda})^2}, \quad (20)$$

where $\mathbf{p}_0$ is the local mean momentum. The corresponding single-particle energy is

$$\varepsilon(\mathbf{r},\mathbf{p}) = \frac{p^2}{2m} + a\frac{n}{n_0} + b(\frac{n}{n_0})^\sigma + c\frac{n}{n_0}\frac{1}{1+(\frac{\mathbf{p}-\mathbf{p}_0}{\Lambda})^2} + c\frac{n}{n_0}\left\langle\frac{1}{1+(\frac{\mathbf{p}-\mathbf{p}_0}{\Lambda})^2}\right\rangle_p . \quad (21)$$

For static nuclear matter $\mathbf{p}_0$ vanishes and the last term of Eq. (21) can be evaluated at zero temperature to give

$$\varepsilon^0(\mathbf{r};n) = 3c\frac{n}{n_0}\left(\frac{\Lambda}{p_F}\right)^3\left[\frac{p_F}{\Lambda} - \tan^{-1}(\frac{p_F}{\Lambda})\right]. \quad (22)$$

To ensure proper ground-state behavior, the parameters of the approximate form of the interaction used in this section need to be fitted to ground-state nuclear matter properties. The parameters in Eq. (20) are chosen as $a = -144.9$ MeV, $b = 203.3$ MeV, $\sigma = 1.17$, $c = -75$ MeV, and $\lambda = 1.5$ [10]. This yields $E/A = -16$ MeV, $n_0 = 0.163$ fm^{-3}, $K_{T=0}(n = n_0) = 215$ MeV. As demon-

strated in Sec. III, the full MDYI becomes repulsive at large kinetic energies. The approximate form with the above parameter set does not become repulsive, and the potential goes to zero at large kinetic energies [36]. This difference may be important for the description of highly nonequilibrium properties, but it is not expected to lead to strong effects in equilibrium situations. Thus our following conclusions about the EOS based on Eq. (21) will approximately hold for both parametrizations.

The single-particle energy (21) can be decomposed into a momentum-dependent and a momentum-independent part, and for static nuclear matter ($\mathbf{p_0} = 0$) we can write

$$\begin{aligned}\varepsilon(\mathbf{r},\mathbf{p}) &= \frac{p^2}{2m} + c\frac{n}{n_0}\frac{1}{1+(\frac{\mathbf{p}}{\Lambda})^2} + a\frac{n}{n_0} \\ &\quad + b(\frac{n}{n_0})^\sigma + c\frac{n}{n_0}\left\langle \frac{1}{1+(\frac{\mathbf{p}}{\Lambda})^2}\right\rangle_p \\ &= \frac{p^2}{2m} - c\frac{n}{n_0}\frac{p^2}{p^2+\Lambda^2} + a'\frac{n}{n_0} \\ &\quad + b(\frac{n}{n_0})^\sigma + c\frac{n}{n_0}\left\langle \frac{1}{1+(\frac{\mathbf{p}}{\Lambda})^2}\right\rangle_p ,\end{aligned} \tag{23}$$

where $a' = a + c$. Using the result (22), the last term in (23) can be separated into a zero-temperature and a T-dependent part as

$$\begin{aligned}&c(\frac{n}{n_0})\left\langle \frac{1}{1+(\frac{\mathbf{p}}{\Lambda})^2}\right\rangle_p \\ &\quad = \varepsilon^0(\mathbf{r};n) + \frac{c}{n_0}\int d^3p \frac{f(\mathbf{p}) - f^{\text{Fermi}}_{T=0}(\mathbf{p})}{1+(\frac{\mathbf{p}}{\Lambda})^2} .\end{aligned} \tag{24}$$

According to the usual convention, the density-dependent, $T = 0$ part of the single-particle energy, $\varepsilon(\mathbf{r},\mathbf{p})$, will be referred to as the compressional energy:

$$\begin{aligned}\varepsilon_{\text{comp}}(\mathbf{r};n) &= a'(\frac{n}{n_0}) + b(\frac{n}{n_0})^\sigma + \varepsilon^0(\mathbf{r};n) \\ &= a'\frac{n}{n_0} + b(\frac{n}{n_0})^\sigma \\ &\quad + 3c\frac{n}{n_0}\left(\frac{\Lambda}{p_F}\right)^3\left[\frac{p_F}{\Lambda} - \tan^{-1}(\frac{p_F}{\Lambda})\right] .\end{aligned} \tag{25}$$

In addition to the compressional energy, the total single-particle energy contains a density- and temperature-dependent (thermal) part, which, however, does not depend on the momentum,

$$\varepsilon_{\text{therm}}(\mathbf{r};n,T) = \frac{c}{n_0}\int d^3p \frac{f(\mathbf{p}) - f^{\text{Fermi}}_{T=0}(\mathbf{p})}{1+(\frac{\mathbf{p}}{\Lambda})^2} , \tag{26}$$

and a momentum-dependent part:

$$\varepsilon_{\text{mom}}(\mathbf{r},\mathbf{p}) = p^2\left[\frac{1}{2m} - c(\frac{n}{n_0})\frac{1}{p^2+\Lambda^2}\right] . \tag{27}$$

Thus, the total single-particle energy (21) is decomposed into three terms,

$$\varepsilon(\mathbf{r},\mathbf{p}) = \varepsilon_{\text{comp}}(\mathbf{r};n) + \varepsilon_{\text{therm}}(\mathbf{r};n,T) + \varepsilon_{\text{mom}}(\mathbf{r},\mathbf{p}) . \tag{28}$$

The momentum-dependent part of the interaction gives rise to the following distribution:

$$f(p) = N\exp\left[-\frac{1}{T}\left(\frac{p^2}{2m} - c(\frac{n}{n_0})\frac{p^2}{p^2+\Lambda^2}\right)\right] , \tag{29}$$

where N is the value of the distribution function at zero momentum, as it should be.

The momentum distribution (29) is plotted in Fig. 3 for temperature $T = 40$ MeV, and density $n = 4n_0$ (full curve), together with the Maxwell-Boltzmann distribution at the same density and temperature (dash-dotted), and with the "equivalent" Maxwellian (dotted line). The equivalent mass $m^{\text{MB}}_{\text{eq}}$ is fixed by the condition

$$f(p=0) = f^{\text{MB}}_{\text{eq}}(p=0) . \tag{30}$$

This yields

$$m^{\text{MB}}_{\text{eq}}(n,T) = \frac{1}{2\pi T}\left\{\int d^3p \exp\left[-\frac{p^2}{T}\left(\frac{1}{2m} - c\left(\frac{n}{n_0}\right)\frac{1}{p^2+\Lambda^2}\right)\right]\right\}^{2/3} , \tag{31}$$

where we have used the normalization condition for the distribution function.

B. Equivalent mass and effective mass

The equivalent mass $m^{\text{MB}}_{\text{eq}}$ can be related to the usual effective mass m^* (see, e.g., Ref. [37] and references therein) defined by

$$\frac{p}{m^*} = \frac{d}{dp}\varepsilon(\mathbf{r},\mathbf{p};n) . \tag{32}$$

The effective mass is of course momentum dependent, but independent of constant shifts of the energy scale. From Eq. (32) we obtain

$$\frac{p}{m^*} = \frac{p}{m} - c\frac{n}{n_0}\frac{2p\Lambda^2}{(p^2+\Lambda^2)^2} . \tag{33}$$

or

$$\frac{m^*}{m} = \frac{1}{1 - 2cm\frac{n}{n_0}\frac{\Lambda^2}{(p^2+\Lambda^2)^2}} \tag{34}$$

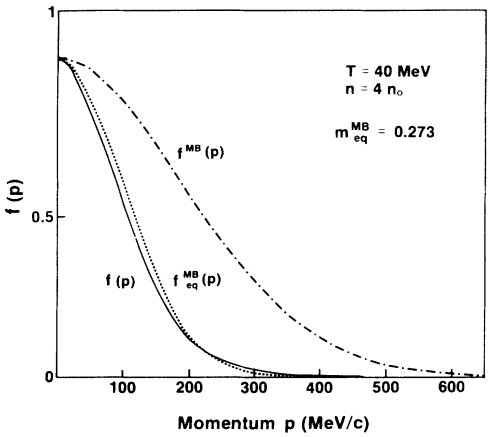

FIG. 3. The momentum distribution in a momentum-dependent mean field (full curve) together with the Maxwell-Boltzmann distribution at the same density and temperature (dash-dotted) and with the "equivalent" Maxwellian (dotted line).

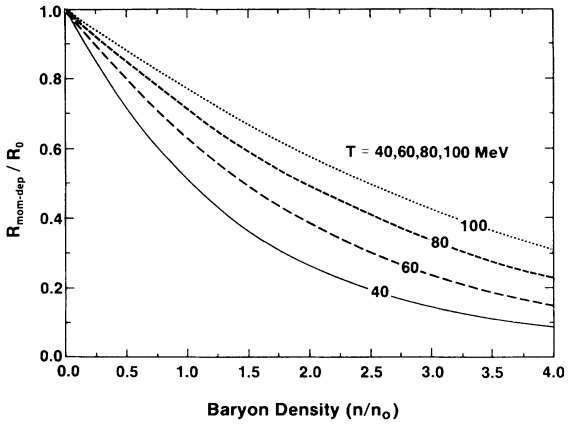

FIG. 5. The ratio of the pion-production rate in the momentum-dependent mean field to the rate without momentum dependence as a function of the density at four temperatures.

We see that the effective mass m^* in the model is equal to the physical mass in the limit of very large momenta, while it approaches the equivalent mass when $p \to 0$.

In Fig. 4 the equivalent mass $m_{\rm eq}^{\rm MB}$ is plotted in units of the free nucleon mass as a function of the density for four different temperatures. At twice standard nuclear matter density and $T = 40$ MeV, one needs an equivalent mass which is about half of the free mass to fit the distribution function in the momentum dependent mean field.

C. Pion production rate

To demonstrate the effect of the momentum dependence on pion production, we calculated the production rate in the equivalent-mass approximation. Here we are interested only in the modification of the rate due to the momentum-dependence. For illustrative purposes we assume pion production through the single delta channel only, and use the free inelastic cross section as parametrized by Cugnon [38] in both the momentum-dependent and momentum-independent calculation.

The pion production rate can be written in the on-shell approximation as [16, 39]

$$R(NN \to \pi X) = \int d^3p\, d^3p' f(\mathbf{p}) f(\mathbf{p}') \sigma(\sqrt{s})\, v_{\rm rel} \ , \tag{35}$$

where $\sigma(\sqrt{s})$ is the inelastic cross section as a function of the center-of-mass energy $s^{1/2}$, and $v_{\rm rel}$ is the relative velocity of the colliding nucleons. In calculating the rate (35) at a given temperature and density, the distribution (19) has been used with the equivalent mass (31) in the momentum-dependent mean field, while the free Maxwell-Boltzmann distribution (18) was utilized in the momentum-independent case.

The application of the equivalent-mass approximation leads to similar expressions for the rates in the momentum-dependent mean field ($R_{\rm mom\text{-}dep}$) and in the free case (R_0). The ratio of these quantities, $R_{\rm mom\text{-}dep}/R_0$ is shown in Fig. 5 for four different temperatures as a function of the density. The rate in the momentum-dependent mean field is significantly below what is expected without momentum dependence even at standard nuclear matter density at not-too-high temperatures. The effect is enhanced as the density is increased to several times the standard density. Since in-medium modified cross sections do not appear in general to deviate from their free values by more than a factor of 2 [40], we expect that this effect remains important when in-medium modifications are taken into account. It should be noted, however, that here we presented an equilibrium calculation for illustration only; a more dynamical calculation in the presence of momentum dependence can be carried out along the lines of Ref. [41].

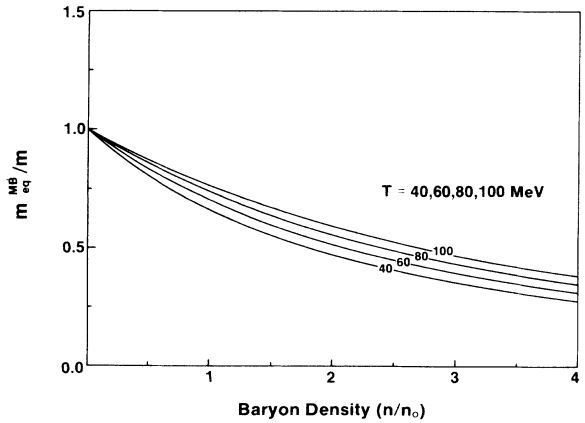

FIG. 4. The equivalent mass in units of the free nucleon mass as a function of the density for four values of the temperature.

V. EQUATION OF STATE

In order to utilize the momentum-dependent interaction in practical applications, the equation of state (EOS) needs to be evaluated [23, 11]. We turn to this task next. It is important to emphasize that, due to the change of the equilibrium momentum distribution, the thermal part of the EOS will be modified. For instance, the incompressibility [given in Eq. (15) for MDYI at $T = 0$] can be evaluated in the present approximation at sufficiently high temperature, and will increase more rapidly with temperature in the presence of the momentum-dependent interaction than without momentum dependence.

To obtain the correction to the EOS relative to a noninteracting system of nucleons, we apply thermodynamic perturbation theory [42]. The free energy of the system is calculated as

$$F = F_0 + < V > - \frac{1}{2T}\left\langle (V - < V >)^2 \right\rangle + \cdots , \qquad (36)$$

where $< V >$ is the average of the interaction energy over the phase space. We take the kinetic energy to determine the zeroth-order approximation, F_0. Only the first nonvanishing correction will be evaluated here, in accordance with the approximations made earlier in the momentum-independent part of the interaction energy.

With the kinetic energy as the single-particle contribution, $E = \sum_{i=1}^{A} p_i^2/2m$, the zeroth order of the free energy can be calculated as

$$F_0 = -T \ln Z_0 = -T \ln \left\{ \int' d\Gamma \, e^{-E/T} \right\} , \qquad (37)$$

where Z_0 is the canonical partition function and $\int' d\Gamma$ accounts for the proper Boltzmann counting in the phase-space integral. The average of the potential energy over the phase space is given by

$$< V >= \frac{\int' d\Gamma \, V}{\int' d\Gamma} = e^{(F_0 - E)/T} \int' d\Gamma \, V \quad . \qquad (38)$$

The calculation is carried out in the Appendix. We obtain simple expressions for the relevant thermodynamic quantities, which do not require more than the error function to be numerically evaluated. In particular, for the pressure we get

$$P(n,T) = nT + \frac{an^2}{2n_0} + \frac{b\sigma}{\sigma+1}\frac{n^{\sigma+1}}{n_0^{\sigma}} + c\frac{n^2}{n_0}\left.\frac{\partial I(n,T)}{\partial n}\right|_T , \qquad (39)$$

where the integral $I(n,T)$ is defined in Eq. (A7).

The EOS is plotted in Fig. 6. The solid lines display the pressure as a function of the density calculated in the present model for temperatures $T = 40$ MeV [Fig. 6(a)] and $T = 100$ MeV [Fig. 6(b)]. The momentum-dependent results are compared to the EOS in the momentum-independent SBKD parametrization [32] (dashed line). It is expected that the Maxwell-Boltzmann approximation breaks down at some density for any given temperature. We associate the fact that the momentum-dependent result falls below the SBKD curve with this unphysical feature of our approximation at high densities, and conclude from Fig. 6 that the present approximation is not applicable beyond $\approx 2n_0$ at $T = 40$ MeV, and beyond $\approx 5n_0$ at $T = 100$ MeV. For the discussion of the quark-gluon phase transition in our approximation it will be sufficient to focus on temperatures above $T \approx 80$ MeV and not too high densities.

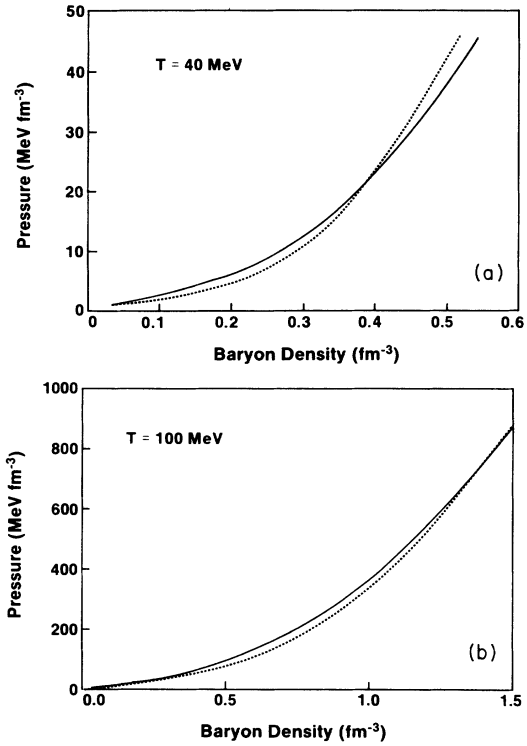

FIG. 6. The equation of state for temperatures (a) $T = 40$ MeV and (b) $T = 100$ MeV in the present model (full curves) and in the momentum-independent SBKD (dashed lines). The fact that the momentum-dependent pressure falls below the SBKD pressure at high densities is associated with the Maxwell-Boltzmann approximation (see text).

VI. PHASE TRANSITION TO THE QUARK-GLUON PLASMA

Ideally, a phase transition should be described by a model which possesses both phases. To what extent and in what sense QCD admits such a phase transition is being investigated. Soliton-matter models give an indication of the transition [43–45]. For our present investigation, where we wish to use the EOS discussed in Sec. V for the hadron phase, we adopt a bag-model EOS for the description of the quark phase. The bag model exhibits two major features of QCD: asymptotic freedom and confinement. It has been used in the past with several versions of the hadronic EOS, not including the effects of momentum dependence [46–49]. Here we follow Ref. [49], which demonstrated that the phase diagram is rather sensitive to the hadronic EOS, while variations of the quark EOS typically give smaller effects, the bag constant B being

the most important quantity in this regard.

We calculated the phase diagram for the SBKD interaction (no momentum dependence) and for the momentum-dependent mean field treated in first-order thermodynamic perturbation theory. To ensure proper low-density behavior, an ideal massless pion gas with free energy

$$F_\pi(T) = -\frac{\pi^2}{30}T^4\Omega \tag{40}$$

(where Ω is the total volume of the system) was added to the hadronic EOS in both parametrizations.

In zeroth-order perturbation theory for two flavors of massless quarks, the bag-model QGP pressure P_Q can be written in terms of the temperature T, the baryochemical potential μ, and the bag constant as

$$P_Q = \frac{37\pi^2}{90}T^4 + \frac{1}{9}\mu^2T^2 + \frac{1}{162\pi^2}\mu^4 - B\,. \tag{41}$$

To obtain the phase boundaries we solve the Gibbs criteria, which can be reduced at any given temperature T to the equation

$$P_H(n,T) = P_Q(\mu(n,T),T)\,, \tag{42}$$

where $P_H = P + P_\pi$, with P being the baryon pressure (39) and P_π the pion pressure from the free energy (40).

The phase diagram of the first-order phase transition observed in the model for $B = 123$ MeV/fm^3, and without perturbative corrections to the quark phase is shown in Fig. 7. When discussing Fig. 7, it should be kept in mind that only an ideal massless pion gas was added to the nucleons in the hadronic phase. This is a minimum requirement for the phase diagram to show proper behavior as $n \to 0$. The inclusion of further mesons and resonances may lead to quantitative changes at small densities. With respect to baryonic resonances, the inclusion of antinucleons [49,50] and Δ resonances [49] changes the results by less than 1%.

Figure 7(a) reflects the softness of SBKD. Starting from zero temperature we note that the hadronic phase boundary starts at $n = 2.1$ fm^{-3} at $T = 0$ (not shown). A "critical point" is reached at $T_{c3} = 105$ MeV and $n_{c3} \approx 1.1$ fm^{-3}. With the density decreasing, equilibrium can only be maintained at a lower temperature, due to the softness of SBKD. There is an unusual mixed phase, where both temperature and density decrease, until the pressure of the pion gas takes over. This results in the critical points at $T_{c2} = 97$ MeV, $n_{c2} \approx 0.45$ fm^{-3}, and $T_{c1} = 126$ MeV at zero baryon density.

The phase diagram with the momentum-dependent hadronic EOS [Fig. 7(b)] approximates the SBKD result for $n \approx 0$, where the pion gas dominates. At $T = 0$ the two equations of state are identical. In the intermediate region, a flat plateau with a narrow region of mixed phase develops at $T \approx 86$ MeV. It is interesting to note that, although the pressures of the two hadronic EOS's are approximately equal at $T = 100$ MeV and $n = 1.4$ fm^{-3}, the corresponding chemical potentials are different by about 50%. This is nicely reflected by the fact that the phase boundaries are not identical either.

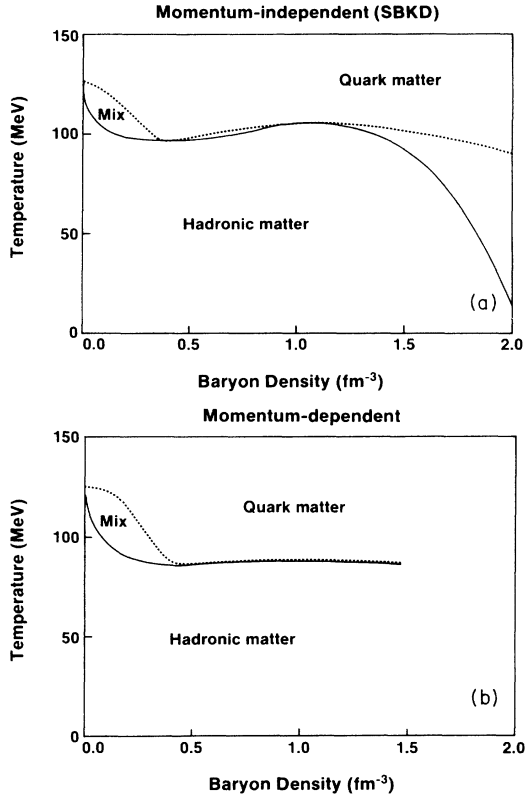

FIG. 7. Phase diagram for the transition to the quark phase with (a) SBKD and (b) in the present approximation. The full line represents the boundary of the hadronic phase; dashes give the boundary of the quark phase. A mixed phase is found between the full and the dashed lines. The $n = 0$ "critical point" is completely determined by the pion gas and the bag constant, and is identical in temperature value for (a) and (b).

The hadronic-side boundary of the mixed phase is about 10% lower at $n = 1.4$ fm^{-3} for MDYI than for SBKD. Since the Boltzmann approximation is not valid at high densities and low temperatures, the phase diagram cannot be fully calculated in our simple (almost analytic) approximation. However, we have carried out a calculation of the shock adiabates, which determine the density and temperature in the compression stage of a nuclear collision, along the lines of Ref. [49]. This computation indicates that the density does not become too high in nuclear collisions, and therefore the Boltzmann approximation is sufficient from the point of view of describing the QGP phase transition in heavy-ion experiments.

VII. CONCLUDING REMARKS

In the present work, we have studied the equation of state of nuclear matter with a momentum-dependent effective interaction. In order to afford a description which leads to vanishing interaction between nucleons of large relative momenta, we chose the momentum-dependent Yukawa interaction (MDYI) as the specific interaction used in this study. No attempt has been made here to

provide a theory of nuclear matter starting from a realistic interaction. A first step to compare the MDYI to more elaborate nuclear matter calculations [51, 52] was taken in Ref. [32].

We have presented analytical results for the zero-temperature optical potential and incompressibility. The results for the optical potential appear to agree well with optical-model analyses of reaction cross sections in a wide energy range indicating the usefulness of the MDYI in studies at high energies. The effective incompressibility is growing faster than linear with the density at zero temperature.

To make further progress, we have used a simplified version of the MDYI to obtain the momentum distribution in a momentum-dependent mean field. An equivalent mass was introduced to simplify numerical calculations. We have demonstrated that the modified momentum distribution implied by the momentum dependence reduces equilibrium pion-production rates. We have studied the equation of state with the simplified interaction, including the phase transition to a quark-gluon plasma described by a bag-model equation of state. It was found that the momentum dependence decreases the temperature at which the quark phase can be reached in the model. The region of the mixed phase is also decreased, which may be an advantage experimentally.

The equilibrium pion-production rates obtained here indicate that it is important that full dynamical pion and dilepton-production calculations be carried out with the momentum-dependent mean field. Our conclusions on the phase transition are based on a bag-model equation of state for the quark phase, and on no meson resonances other than the pion in the hadronic phase. Under these assumptions we found a reduction of the critical temperature at finite density due to the momentum dependence. Further studies of the phase transition are needed in a framework that naturally encompasses both the hadronic and quark phases. It will also be interesting to see whether our simplifying approximation used in the equation-of-state and phase-transition studies can be relaxed in order to carry out similar calculations with the full complexity of the momentum-dependent Yukawa interaction. We are presently pursuing these aspects.

ACKNOWLEDGMENTS

We are grateful to B. Friman, Gy. Kluge, J. Knoll, V.K. Mishra, and G.M. Welke for stimulating discussions. This work was supported in part by the U.S. DOE under Grants No. DE-FG02-86ER40251 and No. DE-FG02-87ER40328, the U.S. NSF under Grant No. INT-8813351, the Natural Sciences and Engineering Research Council of Canada, the FCAR fund of Quebec, and by the Norwegian Research Council for Science and Humanities (NAVF).

APPENDIX

In this Appendix we calculate the free energy (36) through first order. We make the spin-isospin degeneracy of nucleons, $g = 4$, and $\hbar$ explicit, while keeping $c = k = 1$ units. For the zeroth order of the free energy, F_0 of Eq. (37), we take the kinetic energy $E = \sum_{i=1}^{A} p_i^2/2m$, as the single-particle contribution to get

$$F_0 = -T \ln \left\{ \int' d\Gamma e^{-E/T} \right\} = -AT + AT \ln \left[\frac{n(2\pi\hbar)^3}{g(2\pi m T)^{3/2}} \right] . \tag{A1}$$

Next we evaluate the average of the potential energy over the phase space (38). For the full momentum dependence (7) this can be written as

$$< V >= e^{(F_0-E)/T} \frac{1}{A!} \frac{1}{(2\pi\hbar)^{3A}} \int d^{3A}r d^{3A}p \left\{ \frac{1}{2} \sum_{i \neq j} \left[v_{ij}^{(0)}(\mathbf{r}_i - \mathbf{r}_j) + \frac{2c}{n_0} \frac{\delta(\mathbf{r}_i - \mathbf{r}_j)}{1 + (\frac{\mathbf{p}_i - \mathbf{p}_j}{\Lambda})^2} \right] \right\} + \cdots . \tag{A2}$$

Performing the major part of the phase-space integrals leads to factors cancelled by $e^{(F_0-E)/T}$. The sums over identical terms give factors of $A(A-1)$. The resulting expression is

$$< V >= \frac{A(A-1)}{2\Omega^2} \int d^3r\, d^3r' v_{ij}^{(0)}(\mathbf{r}_i - \mathbf{r}_j) + \frac{A(A-1)\, c}{n_0\, \Omega\, (2\pi m T)^3} \int d^3p d^3p' \frac{e^{-p^2/2mT}\, e^{-p'^2/2mT}}{1 + (\frac{\mathbf{p}-\mathbf{p}'}{\Lambda})^2} , \tag{A3}$$

where Ω is the total volume of the system.

We now assume a sufficiently large system ($A \gg 1$) with a constant (position-independent) density n. Then $(A-1)/\Omega \approx A/\Omega = n$. Further, we specialize to the MDYI potential energy density (9) to get

$$< V >= \Omega \left[\frac{a}{2} \frac{n^2}{n_0} + \frac{b}{\sigma+1} \frac{n^{\sigma+1}}{n_0^{\sigma}} + \frac{c\, n^2}{n_0 (2\pi m T)^3} \int d^3p\, d^3p' \frac{e^{-p^2/2mT}\, e^{-p'^2/2mT}}{1 + [(\mathbf{p} - \mathbf{p}')/\Lambda]^2} \right] . \tag{A4}$$

Observing that $f_0(p) = \frac{n(2\pi\hbar)^3}{g(2\pi m T)^{3/2}} e^{-p^2/2mT}$, expression (A4) can be reduced to

$$< V >= \Omega \left[\frac{a}{2}\frac{n^2}{n_0} + \frac{b}{\sigma+1}\frac{n^{\sigma+1}}{n_0^\sigma} + \frac{c}{n_0}\frac{g^2}{(2\pi\hbar)^6}\int d^3p\, d^3p' \frac{f_0(\mathbf{p}) f_0(\mathbf{p}')}{1+(\frac{\mathbf{p}-\mathbf{p}'}{\Lambda})^2} \right]. \tag{A5}$$

To simplify further, we apply the approximations used in Sec. IV, i.e., we replace one of the momenta in Eq. (A5) by its average, $\mathbf{p}' \to < \mathbf{p}' >= \mathbf{p}_0$, and assume that $\mathbf{p}_0 = 0$. This leads to

$$< V >= \Omega \left[\frac{a}{2}\frac{n^2}{n_0} + \frac{b}{\sigma+1}\frac{n^{\sigma+1}}{n_0^\sigma} + c\frac{n}{n_0}\frac{g}{(2\pi\hbar)^3}\int d^3p \frac{f_0(\mathbf{p})}{1+(\frac{\mathbf{p}}{\Lambda})^2} \right]. \tag{A6}$$

Let us introduce the notation $I(n,T)$ for the integral in the last term:

$$I(n,T) \equiv \frac{g}{(2\pi\hbar)^3}\int d^3p \frac{f_0(p)}{1+(\frac{p}{\Lambda})^2}\,. \tag{A7}$$

From (36), (37), and (A6), the total free energy in this approximation is

$$F(n,T) = \Omega\left\{ -nT + nT\ln\left[\frac{n(2\pi\hbar)^3}{g(2\pi m T)^{3/2}}\right] + \frac{an^2}{2n_0} + \frac{b}{\sigma+1}\frac{n^{\sigma+1}}{n_0^\sigma} + c\frac{n}{n_0}I(n,T)\right\}. \tag{A8}$$

The corresponding pressure, entropy, energy, and chemical potential are, respectively,

$$P(n,T) = nT + \frac{an^2}{2n_0} + \frac{b\sigma}{\sigma+1}\frac{n^{\sigma+1}}{n_0^\sigma} + c\frac{n^2}{n_0}\left.\frac{\partial I(n,T)}{\partial n}\right|_T, \tag{A9}$$

$$\frac{S(n,T)}{A} = \frac{5}{2} - \ln\left[\frac{n(2\pi\hbar)^3}{g(2\pi m T)^{3/2}}\right] - \frac{c}{n_0}\left.\frac{\partial I(n,T)}{\partial T}\right|_n, \tag{A10}$$

$$\begin{aligned} E(n,T) &= F + TS \\ &= \Omega\left\{\frac{3}{2}nT + \frac{an^2}{2n_0} + \frac{b}{\sigma+1}\frac{n^{\sigma+1}}{n_0^\sigma} + c\frac{n}{n_0}\left[I(n,T) - T\left.\frac{\partial I(n,T)}{\partial T}\right|_n\right]\right\}, \end{aligned} \tag{A11}$$

$$\mu(n,T) = \left.\frac{\partial(F/\Omega)}{\partial n}\right|_T = \frac{F+P\Omega}{A}\,. \tag{A12}$$

A straightforward calculation yields for the derivatives of the integral $I(n,T)$

$$\left.\frac{\partial I(n,T)}{\partial T}\right|_n = -\frac{3}{2T}I(n,T) + J(n,T), \tag{A13}$$

$$\left.\frac{\partial I(n,T)}{\partial n}\right|_T = \frac{1}{n}I(n,T)\,, \tag{A14}$$

where

$$J(n,T) \equiv \frac{1}{T^2}\frac{g}{(2\pi\hbar)^3}\int d^3p \frac{p^2}{2m}\frac{f_0(p)}{1+(\frac{p}{\Lambda})^2} \tag{A15}$$

is essentially a second moment.

The integrals $I(n,T)$ and $J(n,T)$ can be evaluated to give

$$I(n,T) = 2n\chi^2\left\{1 - \sqrt{\pi}\chi e^{\chi^2}\left[1-\Phi(\chi)\right]\right\}, \tag{A16}$$

$$J(n,T) = \frac{2n\chi^2}{T}\left\{\frac{1}{2} - \chi^2 + \sqrt{\pi}\chi^3 e^{\chi^2}\left[1-\Phi(\chi)\right]\right\}, \tag{A17}$$

where $\chi^2 = \frac{\Lambda^2}{2mT}$ and $\Phi(x) = \frac{2}{\sqrt{\pi}}\int_0^x e^{-t^2}dt$ is the error function.

[1] J.P. Blaizot, Phys. Rep. **64**, 171 (1980).

[2] M.M. Sharma, W.T.A. Borghols, S. Brandenburg, S. Crona, A. van der Woude, and M.N. Harakeh, Phys. Rev. C **38**, 2562 (1988).

[3] H.A. Gustafsson, H.H. Gutbrod, B. Kolb, H. Löhner, B. Ludewigt, A.M. Poskanzer, T. Renner, H. Riedesel, H.G. Ritter, A. Warwick, F. Weik, and H. Wieman, Phys. Rev. Lett. **52**, 1590 (1984).

[4] G.F. Bertsch, H. Kruse, and S. DasGupta, Phys. Rev. C **29**, 673 (1984).

[5] H. Kruse, B.V. Jacak, and H. Stöcker, Phys. Rev. Lett. **54**, 289 (1985).

[6] E. Baron, J. Cooperstein, and S. Kahana, Phys. Rev. Lett. **55**, 126 (1985).

[7] E. Baron, H.A. Bethe, G.E. Brown, J. Cooperstein, and S. Kahana, Phys. Rev. Lett. **59**, 736 (1987).
[8] G.E. Brown and E. Osnes, Phys. Lett. **159B**, 223 (1985).
[9] T.L. Ainsworth, E. Baron, G.E. Brown, J. Cooperstein, and M. Prakash, Nucl. Phys. **A464**, 740 (1987).
[10] C. Gale, G.F. Bertsch, and S. Das Gupta, Phys. Rev. C **35**, 1666 (1987).
[11] J. Aichelin, A. Rosenhauer, G. Peilert, H. Stöcker, and W. Greiner, Phys. Rev. Lett. **58**, 1926 (1987).
[12] *The Nuclear Equation of State*, NATO ASI Series, Vol. 216 A&B, Proceedings of the NATO Advanced Study Institute, Peñíscola, 1989, Spain, edited by W. Greiner and H. Stöcker (Plenum, New York, 1989).
[13] G.F. Bertsch and S. Das Gupta, Phys. Rep. **160**, 189 (1988).
[14] G.E. Brown and V. Koch, *Proceedings of the 8th High Energy Heavy Ion Study*, edited by J.W. Harris and G.J. Wozniak, Berkeley, CA, 1987 (Report No. LBL-24580, 29, 1988).
[15] G. Peilert, A. Rosenhauer, T. Rentsch, H. Stöcker, J. Aichelin, and W. Greiner, in [14] (LBL-24580, 43, 1988).
[16] C. Gale and J. Kapusta, Phys. Rev. C **35**, 2107 (1987).
[17] C.M. Ko and L.H. Xia, Phys. Rev. Lett. **62**, 1595 (1989).
[18] G. Fai, Phys. Scr. **T32**, 81 (1990).
[19] J. Aichelin, Phys. Rep. **202**, 233 (1991).
[20] P. Carruthers and F. Zachariasen, Rev. Mod. Phys. **55**, 245 (1983).
[21] E.A. Remler and A.P. Sathe, Phys. Rev. C **18**, 2293 (1978).
[22] T.H.R. Skyrme, Nucl. Phys. **9**, 615 (1959).
[23] H. Jaqaman, A.Z. Mekjian, and L. Zamick, Phys. Rev. C **27**, 2782 (1983).
[24] H.J. Yuan, H.L. Lin, G. Fai, and S.A. Moszkowski, Phys. Rev. C **40**, 1448 (1989).
[25] W.D. Myers and W.J. Swiatecki, Ann. Phys. (N.Y.) **55**, 395 (1969).
[26] W.D. Myers and W.J. Swiatecki, Annu. Rev. Nucl. Part. Phys. **32**, 309 (1982).
[27] W.D. Myers and W.J. Swiatecki, Ann. Phys. (N.Y.) **204**, 401 (1990).
[28] R.G. Seyler and C.H. Blanchard, Phys. Rev. **124**, 227 (1961); **131**, 355 (1963).
[29] J. Randrup and E.D. Medeiros, Nucl. Phys. **A529**, 115 (1991).
[30] W.A. Küpper, G. Wegman, and E.R. Hilf, Ann. Phys. (N.Y.) **88**, 454 (1974).
[31] G.M. Welke, M. Prakash, T.T.S. Kuo, S. Das Gupta, and C. Gale, Phys. Rev. C **38**, 2101 (1988).
[32] C. Gale, G.M. Welke, M. Prakash, S.J. Lee, and S. Das Gupta, Phys. Rev. C **41**, 1545 (1990).
[33] M. Bauer, E. Hernández-Saldaña, P.E. Hodgson, and J. Quintanilla, J. Phys. G **8**, 525 (1982).
[34] A. Bohr and B.R. Mottelson, *Nuclear Structure* (Benjamin, New York, 1969), Vol. 1.
[35] L.G. Arnold *et al.*, Phys. Rev. C **25**, 936 (1982).
[36] V. Koch, GSI Scientific Report No. GSI 1989-1, 1989, p. 109.
[37] J.W. Negele and K. Yazaki, Phys. Rev. Lett. **47**, 71 (1981).
[38] J. Cugnon, D. Kinet, and J. Vandermuelen, Nucl. Phys. **A379**, 553 (1982).
[39] L.H. Xia, C.M. Ko, L. Xiong, and J.Q. Wu, Nucl. Phys. **A485**, 721 (1988).
[40] J. Jiang, D. Keane, J. Cogar, G. Fai, S. Hayasi, C. Hartnack, and H. Stöcker, Phys. Rev. C **43**, 2353 (1991).
[41] C. Gale, Phys. Rev. C **36**, 2152 (1987).
[42] L.D. Landau and E.M. Lifshitz, *Statistical Physics (Part 1)* (Pergamon, New York, 1980).
[43] J. Achtzehnter, W. Scheid, and L. Wilets, Phys. Rev. D **32**, 2414 (1985).
[44] N.K. Glendenning and B. Banerjee, Phys. Rev. C **34**, 1072 (1986).
[45] M.C. Birse, J.J. Rehr, and L. Wilets, Phys. Rev. C **38**, 359 (1988).
[46] V.V. Dixit, H. Satz, and E. Suhonen, Z. Phys. C **14**, 275 (1982).
[47] V.V. Dixit and J. Lodenquai, Phys. Lett. **153B**, 240 (1985).
[48] J. Cleymans, R. Gavai, and E. Suhonen, Phys. Rep. **130**, 217 (1986).
[49] A.K. Holme, E.F. Staubo, L.P. Csernai, E. Osnes, and D. Strottman, Phys. Rev. D **40**, 3735 (1989).
[50] Gy. Kluge, private communication (1991).
[51] B. Friedman and V.R. Pandharipande, Phys. Lett. **100B**, 205 (1981).
[52] B. Friedman, V.R. Pandharipande, and Q.N. Usmani, Nucl. Phys. **A372**, 483 (1981).